National Conference with International Participation
ENGINEERING MECHANICS 2006
Svratka, Czech Republic, May 15 – 18, 2006

paper no.
225

A NONLINEAR BAR ELEMENT WITH VARYING STIFFNESS

R. Ďuriš[*]

Summary: *The contribution is devoted to description of an exact bar element with varying stiffness. The 2nd theory solution is based on the full nonincremental nonlinear (geometric and material) lagrange FEM formulation of the body motion equations. The new shape functions of the bar element have been established with consideration of continuous variation of elasticity and plasticity moduli, yield stress and cross-sectional area. The efficiency and accuracy of the new elements have been compared with the solutions of identical problems using the ANSYS program. New finite element meets exactly all the basic equations of the bar in both the local and global sense. The results obtained with this element are not dependent on the mesh density.*

1. Basic equations

In the static structural nonlinear analysis the equilibrium differential equations are often expressed by the principle of virtual work. These nonlinear equations are usually linearised with consequent rise of inaccuracies, their elimination requires increasing the number of incremental load steps and/or iterations.

In this contribution a new approach to evaluation of equlibrium equations suggested by Murín [3,4] is presented. In this solution no linearisation of the variation of Green-Lagrange strain tensor is used. Thus we can obtain the exact nonlinear nonincremental formulation of the element stiffness matrices. When total Lagrangian formulation is used, nonlinearised equations can be derived from the equlibrium of internal and external work

$$\int_{^0V} {}^tC_{ijrs}\,e_{rs}\,\delta e_{ij}\,dV + \int_{^0V} {}^tC_{ijrs}\left(e_{rs}\,\delta\eta_{ij} + \eta_{rs}\,\delta e_{ij} + \eta_{rs}\,\delta\eta_{ij}\right)dV = \int_{^0A} {}^tf_i\,\delta u_i\,dA + {}^tF_i^k\,\delta u_k \qquad (1)$$

written in conventional notation. After implementation of correspondent approximation of the displacement functions $u_i = \phi_{ik}\,u_i^k$ we can modify equation (1) for FEM requirements in the form

$$\frac{1}{4}\int_{^0V} {}^tC_{ijkl}(\phi_{km,l}+\phi_{lm,k})(\phi_{in,j}+\phi_{jn,i})u_i^m\,dV + \frac{1}{4}\int_{^0V} {}^tC_{ijkl}\,\phi_{pm,k}\,\phi_{pr,l}(\phi_{in,j}+\phi_{jn,i})u_i^m u_i^r\,dV +$$

$$+\frac{1}{2}\int_{^0V} {}^tC_{ijkl}\,\phi_{pr,i}\,\phi_{pn,j}(\phi_{km,l}+\phi_{lm,k})u_i^m u_i^r\,dV + \frac{1}{2}\int_{^0V} {}^tC_{ijkl}\,\phi_{pm,k}\,\phi_{pv,l}\,\phi_{rq,i}\,\phi_{rn,j}\,u_i^m u_i^v u_i^q\,dV = \quad . \quad (2)$$

$$= \int_{^0A} {}^tf_i\,\phi_{in}\,dA + {}^tF_i^n$$

We will get basic relation which can be used for an arbitrary finite element derivation.

---

[*] Rastislav Ďuriš (MSc.): Department of Applied Mechanics, Faculty of Materials Science and Technology, Slovak University of Technology; Paulínska 16; 917 24 Trnava; Slovak Republic; tel.: +421.33 5511 733, fax: +421.33 5511 668; e-mail: rastislav.duris@stuba.sk

Basic equations of the bar element with full nonlinear stiffness matrix were described in previous papers [1,3,4]. These papers are devoted to description of the bar element with constant or varying stiffness in linear elastic load condition. This paper extends this approach to linear elastic-plastic field of loading.

2. The bar element with constant stiffness

After substitution of the straight bar shape functions

$$u(x) = \phi_1 u_i + \phi_2 u_k = \left(1 - \frac{x}{L^0}\right)u_i + \frac{x}{L^0}u_k \tag{3}$$

into (2) we obtain local nonlinear elastic stiffness matrix of the element in following form

$$\mathbf{K} = k_e \begin{bmatrix} 1 & -1 \\ -1 & 1 \end{bmatrix}. \tag{4}$$

where $k_e = \dfrac{A^0 E^0}{L^0}\left[1 + \dfrac{3}{2}(\lambda - 1) + \dfrac{1}{2}(\lambda - 1)^2\right]$ and $\lambda = \dfrac{u_k - u_i}{L^0} + 1$ denotes stretching of the bar. By implementation of the parameter λ, the stiffness matrices become invariant to the rigid body motion [3,4]. The axial stress in the bar element reached before yield stress σ_y can be calculated using formula

$$\sigma_e = -\frac{E^0}{L^0}\left[1 + \frac{3}{2}(\lambda - 1) + \frac{1}{2}(\lambda - 1)^2\right](\lambda - 1)L^0 . \tag{5}$$
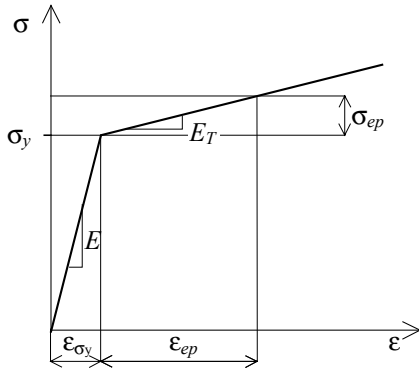

Fig. 1: One-dimensional bilinear stress-strain relationship with hardening

If the axial stress exceeds the yield stress σ_y, it is neccesary to establish new relationship between the stress increment and the strain at the bar. If bilinear stress-strain relation is considered (Fig. 1) and plasticity condition in the bar is reached, it is sufficient to change the linear elastic term k_e in (4) to the elasto-plastic term k_{ep}

$$k_{ep} = \frac{A^0 E^0}{L^0}\left[1 + \frac{3}{2}\left(\lambda - \lambda_{\sigma_y}\right) + \frac{1}{2}\left(\lambda - \lambda_{\sigma_y}\right)^2\right]. \tag{6}$$

The stress in the bar is then equal

$$\sigma = \sigma_y + \sigma_{ep}, \tag{7}$$

where

$$\sigma_{ep} = -\frac{E^0}{L^0}\left[1 + \frac{3}{2}(\lambda - \lambda_{\sigma_y}) + \frac{1}{2}(\lambda - \lambda_{\sigma_y})^2\right](\lambda - \lambda_{\sigma_y})L^0 . \tag{8}$$

and λ_{σ_y} is the bar stretching when yield stress is reached.

A system of nonlinear equations is usually solved using Newton-Raphson method. In this solution process, the full tangent stiffness matrix is required. Local tangent stiffness matrix can be obtained as the derivative of the residual force vector

$$\mathbf{K}_T = \mathbf{K}_L + \mathbf{K}_{NL} + \mathbf{u}^{\mathrm{T}} \frac{\partial \mathbf{K}_{NL}}{\partial \mathbf{u}}. \qquad (9)$$

The elastic and elastic-plastic stiffness matrices $\mathbf{K}_T$ are then expressed by

$$\mathbf{K}_{T_e} = \frac{A^0 E^0}{L^0}\left[1 + 3(\lambda-1) + \frac{3}{2}(\lambda-1)^2\right] \quad \text{and} \quad \mathbf{K}_{T_{ep}} = \frac{A^0 E^0}{L^0}\left[1 + 3(\lambda-\lambda_y) + \frac{3}{2}(\lambda-\lambda_y)^2\right] \quad (10)$$

Typical example of geometric nonlinear behaviour is the three-hinge mechanism (Fig. 4). The dependence displacement vs. internal/global force for linear elastic solution of the bar with uniform cross-section (Fig. 4a) is well known from literature. For bilinear elastic-plastic behaviour this dependence is shown in Fig. 2 and comparison with the linear elastic solution is presented.
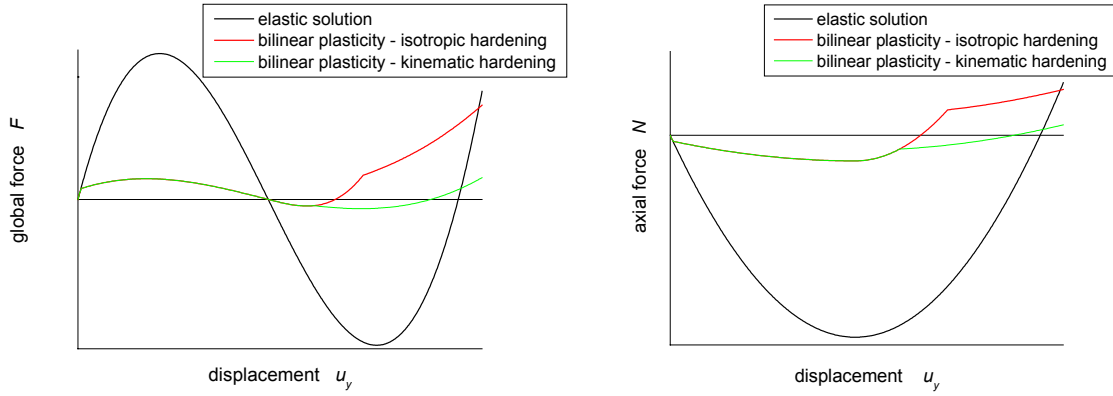
Fig. 2: Example of equilibrium path for linear elastic and bilinear elastic-plastic material properties von Mises two bar structure with constant stiffness

3. The bar element with varying stiffness

The straight bar element with varying stiffness is shown in Fig. 3. The cross-sectional area, elasticity and tangential moduli are defined as the polynomial functions

$$A(x) = A_i\left(1 + \sum_{k=1}^{p}\eta_{Ak}x^k\right); \quad E(x) = E_i\left(1 + \sum_{k=1}^{q}\eta_{Ek}x^k\right) \quad \text{and} \quad E_T(x) = E_{Ti}\left(1 + \sum_{k=1}^{r}\eta_{E_Tk}x^k\right).$$
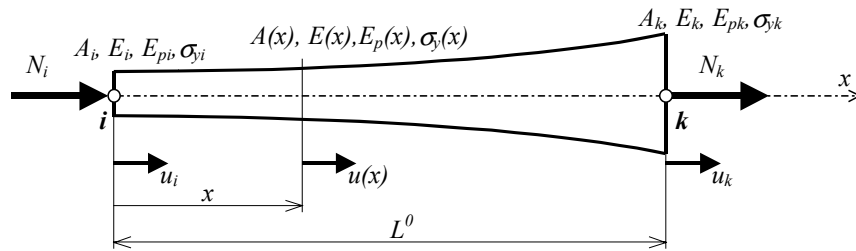

Fig. 3: Bar element with variation of the geometry and material properties in the initial configuration

Then the variation of axial elastic and elastic-plastic stiffnesses can be written as

$$B_e(x) = B_{ei}\left(1 + \sum_{k=1}^{p+q}\eta_{B_ek}x^k\right) = B_{ei}\,\eta_{B_e}(x), \quad B_{ep}(x) = B_{epi}\left(1 + \sum_{k=1}^{p+r}\eta_{B_{ep}k}x^k\right) = B_{epi}\,\eta_{B_{ep}}(x) \quad (11)$$

where $B_{ei} = A_i E_i$, $B_{epi} = A_i E_{Ti}$ and $\eta_{Be}(x)$, $\eta_{Bep}(x)$ describe the variation of the stiffness. If the concept of transfer functions and constants published by Rubin [2] is used to the derivation of the stiffness relation, the axial elastic displacement can be expressed as

$$u(x) = \phi_1 u_i + \phi_2 u_k = \left(1 - \frac{d'_{2B_e}(x)}{d'_{2B_e}}\right) u_i + \frac{d'_{2B_e}(x)}{d'_{2B_e}} u_k \tag{12}$$

where $d'_{2B_e}(x)$ is the first derivative of transfer function, which is given by the relation

$d''_{2B_e}(x) = \dfrac{1}{\eta_{B_e}(x)}$ and $d'_{2B_e} = d'_{2B_e}(x = L^0)$ is the transfer constant.

The term k_e in elastic stiffness matrix (4) has the form

$$k_e = \frac{A_i E_i}{d'_{2B_e}}\left[1 + \frac{3}{2}(\lambda - 1)L^0 \frac{\overline{d'_{2B_e}}}{(d'_{2B_e})^2} + \frac{1}{2}(\lambda - 1)^2(L^0)^2 \frac{\overline{\overline{d'_{2B_e}}}}{(d'_{2B_e})^3}\right] \tag{13}$$

where d'_{2B_e}, $\overline{d'_{2B_e}} = \int_0^{L^0}(d''_{2B_e}(x))^2 dx$, $\overline{\overline{d'_{2B_e}}} = \int_0^{L^0}(d''_{2B_e}(x))^3 dx$ are the transfer constants for elastic loading case, which can be computed by simple numerical algorithm [3,5].

If the axial stress exceeds the yield stress σ_y, the stiffness k_e in equation (4) is changed to k_{ep}

$$k_{ep} = \frac{A_i E_{Ti}}{d'_{2B_{ep}}}\left[1 + \frac{3}{2}(\lambda - \lambda_{\sigma_y})L^0 \frac{\overline{d'_{2B_{ep}}}}{(d'_{2B_{ep}})^2} + \frac{1}{2}(\lambda - \lambda_{\sigma_y})^2(L^0)^2 \frac{\overline{\overline{d'_{2B_{ep}}}}}{(d'_{2B_{ep}})^3}\right] \tag{14}$$

where $d'_{2B_{ep}}, \overline{d'_{2B_{ep}}}, \overline{\overline{d'_{2B_{ep}}}}$ are transfer constants for elastic-plastic loading case.

The internal force and axial stress before yield stress in the bar element, can be calculated using formulae

$$N_e = -\frac{A_i E_{ei}}{d'_{2B_e}}\left[1 + \frac{3}{2}(\lambda - 1)L^0 \frac{\overline{d'_{2B_e}}}{(d'_{2B_e})^2} + \frac{1}{2}(\lambda - 1)^2(L^0)^2 \frac{\overline{\overline{d'_{2B_e}}}}{(d'_{2B_e})^3}\right](\lambda - 1)L^0 \tag{15a}$$

$$\sigma_e = -\frac{E_i}{d'_{2E}}\left[1 + \frac{3}{2}(\lambda - 1)L^0 \frac{\overline{d'_{2E}}}{(d'_{2E})^2} + \frac{1}{2}(\lambda - 1)^2(L^0)^2 \frac{\overline{\overline{d'_{2E}}}}{(d'_{2E})^3}\right](\lambda - 1)L^0 \tag{15b}$$

and for the stress exceeding the elastic limit the internal force and axial stress can be calculated from

$$N_{ep} = -\frac{A_i E_{Ti}}{d'_{2B_{ep}}}\left[1 + \frac{3}{2}(\lambda - \lambda_{\sigma_y})L^0 \frac{\overline{d'_{2B_{ep}}}}{(d'_{2B_{ep}})^2} + \frac{1}{2}(\lambda - \lambda_{\sigma_y})^2(L^0)^2 \frac{\overline{\overline{d'_{2B_{ep}}}}}{(d'_{2B_{ep}})^3}\right](\lambda - \lambda_{\sigma_y})L^0 \tag{16a}$$

$$\sigma_{ep} = -\frac{E_{Ti}}{d'_{2E_T}}\left[1 + \frac{3}{2}(\lambda - \lambda_{\sigma_y})L^0 \frac{\overline{d'_{2E_T}}}{(d'_{2E_T})^2} + \frac{1}{2}(\lambda - \lambda_{\sigma_y})^2(L^0)^2 \frac{\overline{\overline{d'_{2E_T}}}}{(d'_{2E_T})^3}\right](\lambda - \lambda_{\sigma_y})L^0. \tag{16b}$$

where $d'_{2E}, \overline{d'_{2E}}, \overline{\overline{d'_{2E}}}, \ d'_{2E_T}, \overline{d'_{2E_T}}, \overline{\overline{d'_{2E_T}}}$ are transfer constants for Young and tangential moduli functions.

Axial stress in elastic-plastic domain can be calculated using (7) where σ_y is the "average" value of the yield stress function of the bar.

In the elastic state stiffness matrix $\mathbf{K}_T$ is expressed by

$$\mathbf{K}_{Te} = \frac{A_i E_i}{d'_{2B_e}}\left[1 + 3(\lambda - 1)L^0 \frac{\overline{d'_{2B_e}}}{(d'_{2B_e})^2} + \frac{3}{2}(\lambda - 1)^2(L^0)^2 \frac{\overline{\overline{d'_{2B_e}}}}{(d'_{2B_e})^3}\right]\begin{bmatrix} 1 & -1 \\ -1 & 1 \end{bmatrix} \tag{17a}$$

and in the elastic-plastic state by relation

$$\mathbf{K}_{Tep} = \frac{A_i E_{Ti}}{d'_{2B_{ep}}}\left[1 + 3(\lambda - \lambda_{\sigma_y})L^0\,\frac{\overline{d'_{2B_{ep}}}}{(d'_{2B_{ep}})^2} + \frac{3}{2}(\lambda - \lambda_{\sigma_y})^2(L^0)^2\,\frac{\overline{\overline{d'_{2B_{ep}}}}}{(d'_{2B_{ep}})^3}\right]\begin{bmatrix} 1 & -1 \\ -1 & 1 \end{bmatrix}. \quad (17b)$$

The vector of the internal forces can be written

$$\mathbf{F}_{\text{int}} = \begin{bmatrix} N & -N \end{bmatrix}^{\mathrm{T}}. \quad (18)$$

These matrices can be transformed to the global coordinate system using the standard transformation rules.

4. Numerical examples

In the numerical experiments two different solutions were compared. First solution used equations and input values for the bar with constant stiffness (Tab. 1). Second model was created using the bar element with varying stiffness. Selected forms of the variations of cross-sectional area and material properties are shown in Tab. 2 and 3.

Experiments were carried out for bilinear elastic-plastic model of material behaviour with isotropic as well as kinematic hardening.
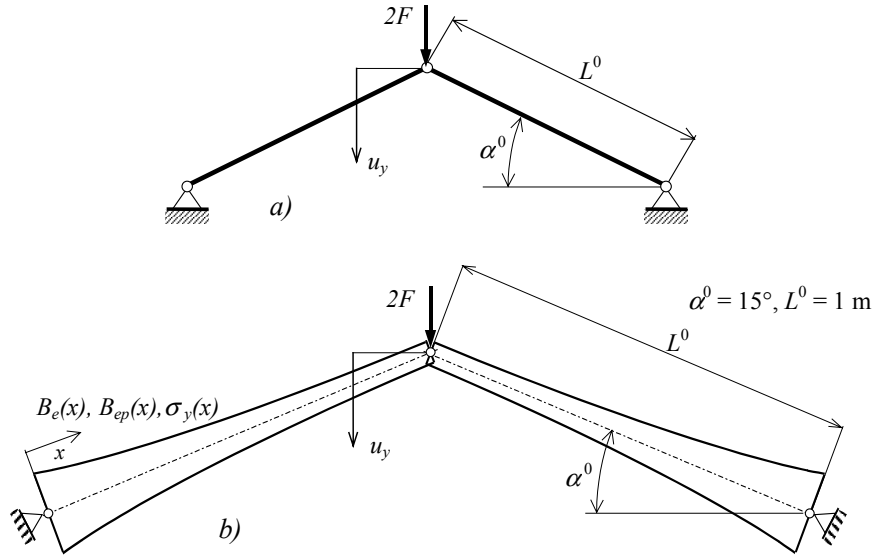
Fig. 4: Two simply supported bars used in numerical examples

To solve our exact nonlinear bar element a code in *MATHEMATICA* software was developed. In the numerical experiments we used two basic approaches to compare accuracy and efficiency of the full exact nonlinear single bar element. To compare exact element results with results obtained by ANSYS, four models were created:

- 1D beam model meshed with 1, 5 and 20 elements (BEAM188 element with tapered cross-sectional area),
- 3D model using SOLID185 element to divide the model into 50 segments of layers of elements.

In all presented solutions the symmetry of the structure was used.

Numerical computations for different types of variability of cross-sectional area and material properties were carried out. Accuracy and coincidence of results of the new exact

element was examined for few ratios B_{max}/B_{min} of the limit values of element stiffness function (11) (see Tab. 3).

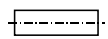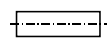Table 1: Cross-section area and material properties for the bar with constant stiffness

	shape	value
A		$A = 0,0015$ m^2
E		$E = 18000.10^6$ Pa; $E_T = 1800.10^6$ Pa; $\sigma_y = 180.10^6$ Pa

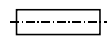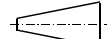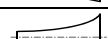Table 2: The geometry and material properties for the bar with varying stiffness
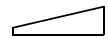
	shape	function	
A1		$A(x) = 0,0015$	[m^2]
A2		$A(x) = 0,001 + 0,0006x$	[m^2]
A3		$A(x) = 0,001 + 0,0007x + 0,0007x^2$	[m^2]
A4		$A(x) = 0,001 + 0,001x + 0,001x^2$	[m^2]
E1		$E(x) = 1,6.10^{11} + 0,4.10^{11}x$	[Pa]
		$E_T(x) = 1,6.10^{10} + 0,4.10^{10}x$	[Pa]
		$\sigma_y(x) = 160.10^6 + 40.10^6x$	[Pa]
E2		$E(x) = 1,5.10^{11} + 0,4.10^{11}x + 0,4.10^{11}x^2$	[Pa]
		$E_T(x) = 1,5.10^{10} + 0,4.10^{10}x+ 0,4.10^{10}x^2$	[Pa]
		$\sigma_y(x) = 150.10^6 + 40.10^6x+ 40.10^6x^2$	[Pa]

Note: For ANSYS solution with one BEAM188 element the following average values of cross-sectional area and material properties were used:

A1	$A_{aver} = 0,0015$ m^2	E1	$E_{aver} = 1,8.10^{11}$ Pa; $E_{T\,aver} = 1,8.10^{10}$ Pa
A2	$A_{aver} = 0,0013$ m^2		$\sigma_{y\,aver} = 180.10^6$ Pa
A3	$A_{aver} = 0,0015833$ m^2	E2	$E_{aver} = 1,833.10^{11}$ Pa; $E_{T\,aver} = 1,833.10^{10}$ Pa
A4	$A_{aver} = 0,0018333$ m^2		$\sigma_{y\,aver} = 183,33.10^6$ Pa

Table 3: Selected combinations and stiffness ratios

element stiffness function	ratio B_{max}/B_{min}
B1 = A1.E1	1,25
B2 = A2.E1	2
B3 = A3.E1	3
B4 = A3.E2	4
B5 = A4.E2	5

5. Results of numerical experiments

Resulting dependence for both the internal force N and global force F on displacement u_y at the common node are given in selected Figs. 5-12 at the end of this contribution.

Figs. 5,6 show results for the bar with constant stiffness and Figs. 7-12 results for the bar with varying stiffness.

The solution with constant stiffness and another five solutions with different variations of stiffness given by various ratios B_{max}/B_{min} were compared. The most exact results were acquired considering isotropic hardening, especially at lower values of ratios B_{max}/B_{min}. Increasing the ratio B_{max}/B_{min} leads to enlargement of differences between exact and ANSYS solutions.

According to results obtained by ANSYS at least five beam elements are necessary to get results comparable with single exact element. ANSYS solid model resulted in nearly identical curves.

6. Conclusions

The main aim of this paper was the comparison of the results of exact nonlinear nonincremental solution. The accuracy and computational efficiency of this new formulation were tested. The results of analyses lead to the following issues:

- the numerical experiments showed very good agreement between the solutions of the exact element and ANSYS results, especially when the isotropic hardening was considered (Figs. 5,7,9,11),
- in ANSYS, the division into at least five beam elements was necessary to achieve accuracy comparable to single exact element,
- considerable differences appeared only for case with kinematic hardening (Figs. 10,12),
- the differences of exact element and ANSYS models results are increasing with the ratio B_{max}/B_{min} greater then six, particularly near the yield stress

These determinations verify high efficiency and accuracy of the developed exact element. Further, the results are independent on the mesh density.

7. Acknowledgement

8. References

[1] J. Murín, V. Kutiš, R. Ďuriš. Non-linear bar with varying stiffness. In: Proceedings of 3rd International Conference on New Trends in Statics and Dynamics of Buildings. Slovak University of Technology, Bratislava, 2004. pp. 91-94, ISBN 80-227-2116-6

[2] H. Rubin. Analytische Lösung linearer Differentialgleichungen mit veränderlichen Koeffizienten und baustatische Anwendung. Bautechnik, Vol. 76, 1999.

[3] V. Kutiš, J. Murín. Bar element with variation of cross-section for geometric non-linear analysis. Journal of Computational and Applied Mechanics, Vol. 6., No. 1., (2005), pp. 83-94, http://mab.mta.hu/~szeidl

[4] Murín, J. Implicit non-incremental FEM equations for non-linear continuum. Strojnícky časopis, Vol. 52, No. 3, 2001.

[5] Murín, J. Metóda konečných prvkov pre prútové a rámové konštrukcie. Bratislava, STU, 1999. (in Slovak)

[6] J. Murín, V. Kutiš. 3D-beam element with continuous variation of the cross-sectional area. Computers & Structures, Vol. 80, 2002, pp. 329/338.
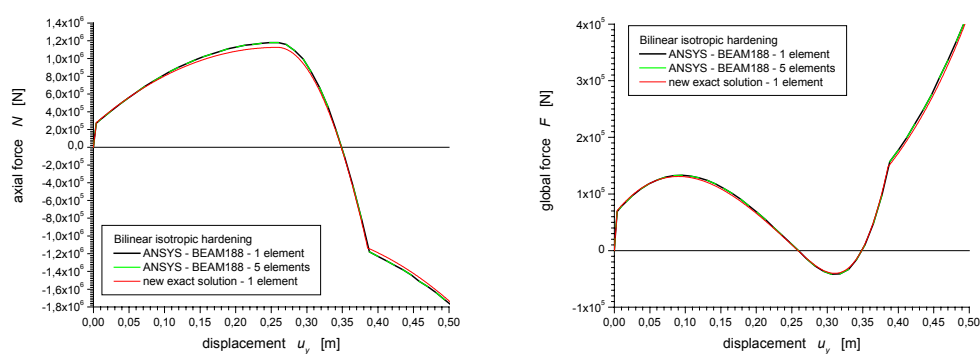
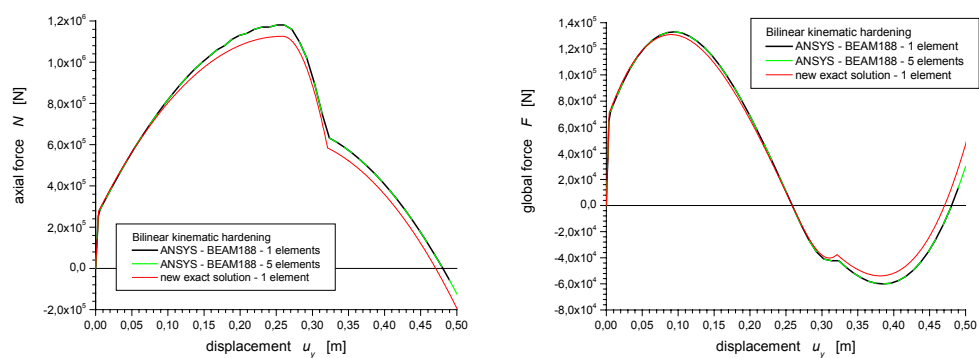Fig. 5: Displacement vs. axial force and global reaction (bar with constant stiffness A.E; isotropic hardening)

Fig. 6: Displacement vs. axial force and global reaction (the bar with constant stiffness A.E; kinematic hardening)
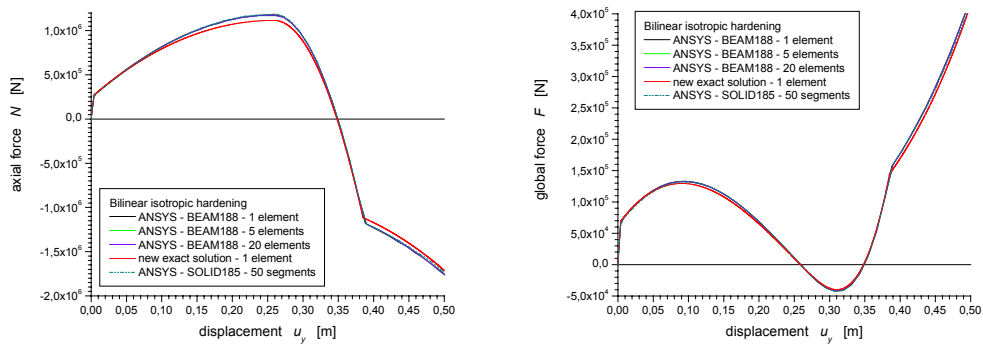
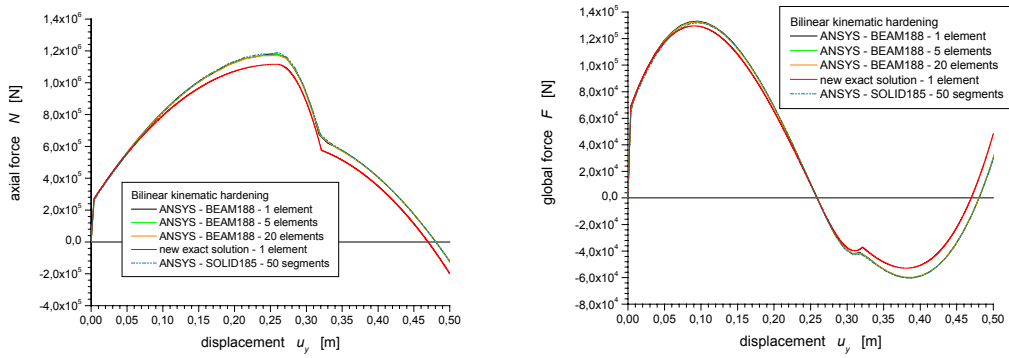Fig. 7: Displacement vs. axial force and global reaction (stiffness function A1.E1; isotropic hardening)

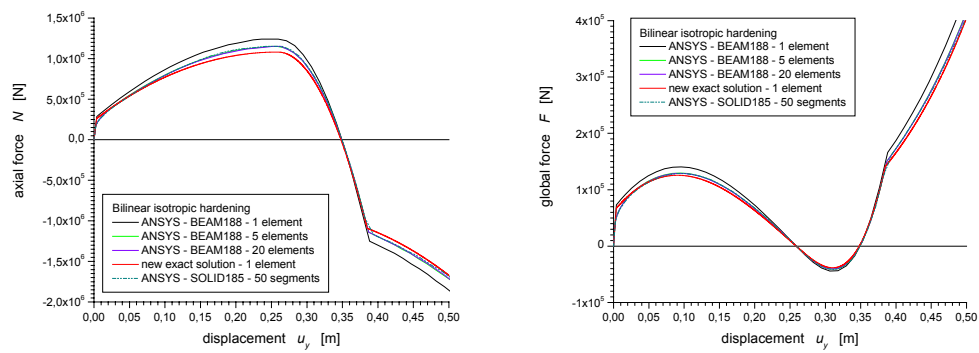Fig. 8: Displacement vs. axial force and global reaction (stiffness function A1.E1; kinematic hardening)

Fig. 9: Displacement vs. axial force and global reaction (stiffness function A3.E1; isotropic hardening)
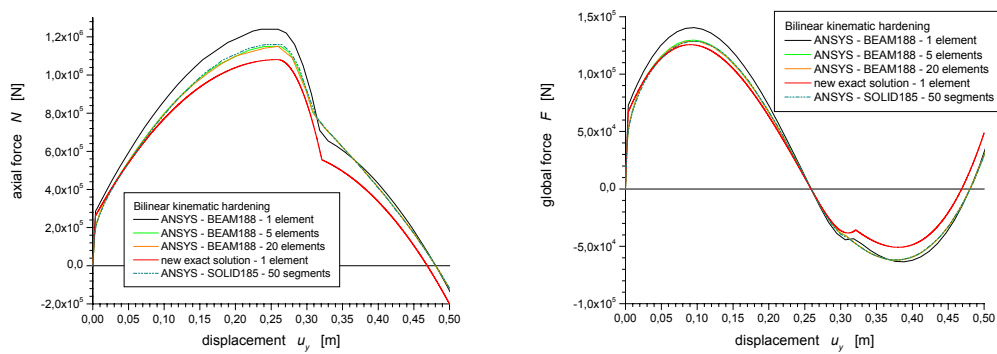

Fig. 10: Displacement vs. axial force and global reaction (stiffness function A3.E1; kinematic hardening)
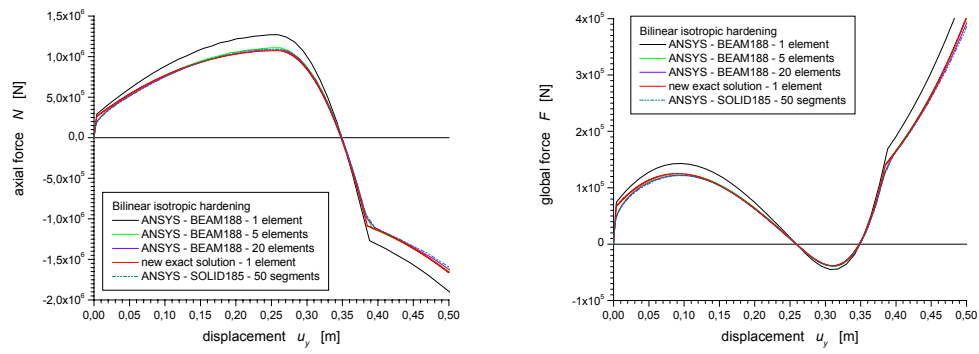
Fig. 11: Displacement vs. axial force and global reaction (stiffness function A3.E2; isotropic hardening)
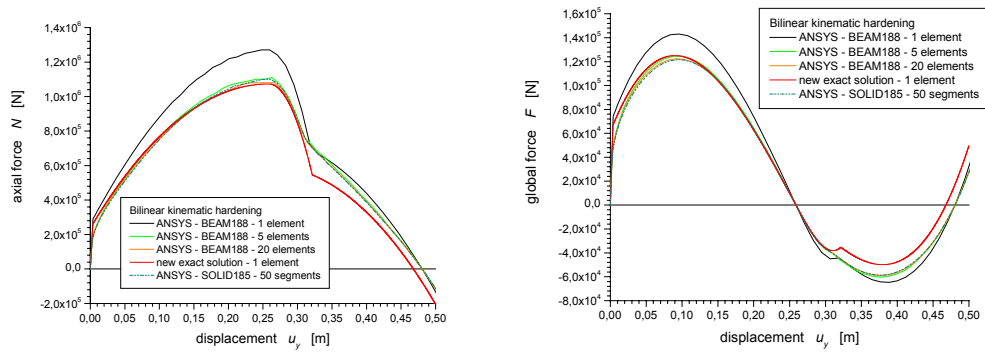

Fig. 12: Displacement vs. axial force and global reaction (stiffness function A3.E2; kinematic hardening)